Nonlinear Dynamics **30:** 323–335, 2002.

Multiple Scales without Center Manifold Reductions for Delay Differential Equations near Hopf Bifurcations

S. L. DAS and A. CHATTERJEE
Mechanical Engineering Department, Indian Institute of Science Bangalore, 560012, India

(Received: 22 January 2002; accepted: 8 August 2002)

Abstract. We study small perturbations of three linear Delay Differential Equations (DDEs) close to Hopf bifurcation points. In analytical treatments of such equations, many authors recommend a center manifold reduction as a first step. We demonstrate that the method of multiple scales, on simply discarding the infinitely many exponentially decaying components of the complementary solutions obtained at each stage of the approximation, can bypass the explicit center manifold calculation. Analytical approximations obtained for the DDEs studied closely match numerical solutions.

Keywords: Delay differential equation, multiple scales, Hopf bifurcation, center manifold.

1. Introduction

The Method of Multiple Scales (MMS) is routinely applied to many weakly nonlinear systems of both Ordinary and Partial Differential Equations (ODEs and PDEs) [1–3]. This method is useful, for example, in the analysis of systems near a Hopf bifurcation, or a resonance, or both.

For Delay Differential Equations (DDEs) or Retarded Functional Differential Equations (RFDEs) in the neighborhood of Hopf bifurcations, many authors suggest first doing a center manifold reduction [4–9]. This reduction eliminates *a priori* the infinitely many exponentially decaying parts of the solution, leaving behind the slowly evolving dynamics on the center manifold.

A possible reason for recommending the explicit center manifold reduction is that DDEs and RFDEs are infinite dimensional, unlike ODEs. However, PDEs are infinite dimensional as well, and the MMS has been applied directly to PDEs (e.g., [10, 11]). Moreover, in [12–14], normal forms of RFDEs are obtained directly without explicitly computing the center manifold.

In this paper, bypassing the preliminary center manifold reduction, as well as the intermediate step of normal forms or a similar calculation on the center manifold, we proceed directly with the coordinate transformation that is of final interest. Using three examples, we demonstrate that the MMS can implicitly eliminate the rapidly decaying parts of the solution, yielding the desired slow flow. For simplicity, we do not at this stage consider additional difficulties such as the degeneracies addressed in [15].

Note that the MMS has previously been directly applied to systems with a time delay (see, e.g., [16–18]), but there the delay terms are multiplied by a small parameter. In other words, the DDE is treated as a slightly perturbed ODE. So, while applying the MMS, the equations to be solved at each order are ODEs and not DDEs. In contrast, in our study the delayed term is not small, and the unperturbed equation is a DDE at a Hopf bifurcation point. For these equations, on applying the MMS we need to solve a DDE at each level.

2. An Autonomous Equation with a Limit Cycle

Consider the equation

$$\dot{y}(t) = -\alpha\, y\left(t - \frac{\pi}{2}\right) - y^3(t), \quad \text{where} \quad \alpha > 0. \tag{1}$$

The characteristic equation for the linearized form of Equation (1) is

$$\lambda + \alpha\, \mathrm{e}^{-(\pi/2)\lambda} = 0. \tag{2}$$

We note that the above equation is equivalent to

$$\bar{\lambda}\, \mathrm{e}^{\bar{\lambda}} + \bar{\alpha} = 0, \tag{3}$$

where $\bar{\lambda} = (\pi/2)\,\lambda$ and $\bar{\alpha} = (\pi/2)\,\alpha$. Equation (3) has been studied elsewhere (see [19, p. 341]), and the following is known:

1. For $0 < \bar{\alpha} < \pi/2$ all the roots have negative real parts.
2. For $\bar{\alpha} > e^{-1}$ there is a root $\bar{\lambda}(\bar{\alpha}) = \gamma(\bar{\alpha}) + i\,\sigma(\bar{\alpha})$ with the following properties:

   (a) It is continuous and differentiable with respect to $\bar{\alpha}$.
   (b) It satisfies $0 < \sigma(\bar{\alpha}) < \pi$, $\sigma(\pi/2) = \pi/2$, $\gamma(\pi/2) = 0$, and $\partial\gamma(\bar{\alpha})/\partial\bar{\alpha}|_{\bar{\alpha}=\pi/2} > 0$.
   (c) Finally, $\gamma(\bar{\alpha}) > 0$ for $\bar{\alpha} > \pi/2$.

Thus, Equation (1) undergoes a Hopf bifurcation at $\bar{\alpha} = \pi/2$ or $\alpha = 1$. At the bifurcation point, $\bar{\lambda} = \pm i\,(\pi/2)$, i.e., $\lambda = \pm i$.

To study the equation close to the bifurcation, we take $\alpha = 1+\varepsilon$ and Equation (1) becomes

$$\dot{y}(t) = -(1+\varepsilon)\, y\left(t - \frac{\pi}{2}\right) - y^3(t), \quad \text{where} \quad 0 < \varepsilon \ll 1. \tag{4}$$

As is generically true near Hopf bifurcations, the above equation has a periodic solution of amplitude proportional to $\sqrt{\varepsilon}$. Accordingly, we write

$$y = \sqrt{\varepsilon}\, x.$$

Equation (4) becomes

$$\dot{x}(t) = -x\left(t - \frac{\pi}{2}\right) - \varepsilon\left[x\left(t - \frac{\pi}{2}\right) + x^3(t)\right]. \tag{5}$$

For Equation (5), a Hopf bifurcation occurs at $\varepsilon = 0$ and a stable periodic solution exists for small $\varepsilon > 0$.

For $\varepsilon = 0$ (i.e., $\alpha = 1$), Equation (5) is linear, and so has a general solution in the form of an infinite linear combination of terms of the form $\mathrm{e}^{\lambda t}$. Of these λs, as discussed above, two are $\pm i$, while all others have negative real parts. Thus, after transients die out exponentially fast, we are left with

$$x(t) = A\sin t + B\cos t, \tag{6}$$

where A and B are arbitrary constants. In what follows, we will treat Equation (6) as the complementary solution to Equation (5) with $\varepsilon = 0$. In this way, we will implicitly remove all the exponentially decaying parts of the solution, and an explicit center manifold calculation will be unnecessary.

To apply the MMS, we begin as usual by defining the multiple time scales: these are t, the original time scale; $T_0 = \varepsilon\, t$; $T_1 = \varepsilon^2\, t$; $T_2 = \varepsilon^3\, t$, and so on. The solution to Equation (5) is assumed to be of the form (retaining four time scales)

$$x(t) = X(t, T_0, T_1, T_2). \tag{7}$$

We assume further that the solution can be expanded in powers of ε, as

$$X(t, T_0, T_1, T_2) = X_0(t, T_0, T_1, T_2) + \varepsilon\, X_1(t, T_0, T_1, T_2) + \varepsilon^2\, X_2(t, T_0, T_1, T_2) + \cdots. \tag{8}$$

Substituting the above expression (Equation (8)) in Equation (5), we obtain

$$\begin{aligned} &\frac{\partial X_0}{\partial t} + \varepsilon \left(\frac{\partial X_1}{\partial t} + \frac{\partial X_0}{\partial T_0} - \frac{\pi}{2} \frac{\partial X_0}{\partial T_0} \left(t - \frac{\pi}{2} \right) \right) \\ &\quad = -X_0 \left(t - \frac{\pi}{2} \right) - \varepsilon \left[X_1 \left(t - \frac{\pi}{2} \right) + X_0 \left(t - \frac{\pi}{2} \right) + X_0^3(t) \right] + \mathcal{O}(\varepsilon^2), \end{aligned} \tag{9}$$

where the lengthy higher order terms have not been displayed. To lowest order, Equation (9) becomes

$$\frac{\partial X_0}{\partial t} = -X_0 \left(t - \frac{\pi}{2} \right). \tag{10}$$

The solution to Equation (10) (by Equation (6)) has the form

$$X_0 = A \sin t + B \cos t, \tag{11}$$

where $A = A(T_0, T_1, T_2)$ and $B = B(T_0, T_1, T_2)$. Henceforth, for brevity, we will write $A(T_0, T_1, T_2)$ and $B(T_0, T_1, T_2)$ simply as A and B, respectively.

Substituting Equation (11) into Equation (9) and simplifying, we obtain the following equation at the next order:

$$\frac{\partial X_1}{\partial t} + X_1 \left(t - \frac{\pi}{2}, T_0, T_1, T_2 \right) + P_1 \sin t + P_2 \cos t + P_3 \sin 3t + P_4 \cos 3t = 0, \tag{12}$$

where P_1, P_2, P_3 and P_4 are given by the following:

$$P_1 = \frac{3}{4} A^3 - \frac{\pi}{2} \frac{\partial B}{\partial T_0} + \frac{\partial A}{\partial T_0} + \frac{3}{4} A\, B^2 + B,$$

$$P_2 = \frac{\pi}{2} \frac{\partial A}{\partial T_0} - A + \frac{3}{4} A^2\, B + \frac{3}{4} B^3 + \frac{\partial B}{\partial T_0},$$

$$P_3 = \frac{3}{4} A\, B^2 - \frac{1}{4} A^3,$$

and

$$P_4 = \frac{1}{4} B^3 - \frac{3}{4} A^2 B.$$

To avoid the occurrence of secular terms in the solution, the coefficients of $\sin t$ and $\cos t$ in Equation (12) are set to zero, i.e., $P_1 = 0$ and $P_2 = 0$. From these, we obtain $\partial A/\partial T_0$ and $\partial B/\partial T_0$, and Equation (12) itself reduces to

$$\frac{\partial X_1}{\partial t} + X_1\left(t - \frac{\pi}{2}, T_0, T_1, T_2\right) + \left(\frac{3}{4} A B^2 - \frac{1}{4} A^3\right) \sin 3t$$
$$+ \left(\frac{1}{4} B^3 - \frac{3}{4} A^2 B\right) \cos 3t = 0. \tag{13}$$

Since we are not solving a specific initial value problem, we omit the homogeneous solution (see, e.g., [1]) and assume the solution to Equation (13) to simply be of the form

$$X_1 = C \sin 3t + D \cos 3t, \tag{14}$$

where, once again, we have implicitly dropped the infinitely many exponentially decaying solutions. To determine the coefficients C and D, Equation (14) is substituted into Equation (13); then C and D are easily seen to be

$$C = -\frac{1}{16} B^3 + \frac{3}{16} A^2 B, \quad D = \frac{3}{16} A B^2 - \frac{1}{16} A^3.$$

The results obtained so far, including the expressions for $\partial A/\partial T_0$ and $\partial B/\partial T_0$, are now substituted into Equation (9) to obtain the differential equation for X_2 at $\mathcal{O}(\varepsilon^2)$. That equation also has forcing terms potentially containing $\sin t$ and $\cos t$ which, if present, give rise to secular terms in the solution. Accordingly, and as before, we set the coefficients of $\sin t$ and $\cos t$ in the X_2 equation equal to zero. We then obtain two equations involving $\partial A/\partial T_1$ and $\partial B/\partial T_1$.

The above procedure can in principle be continued indefinitely (to any order). Finally, the equations for $\dot{A}$ and $\dot{B}$ are given by

$$\dot{A} = \varepsilon \frac{\partial A}{\partial T_0} + \varepsilon^2 \frac{\partial A}{\partial T_1} + \mathcal{O}(\varepsilon^3) \quad \text{and} \quad \dot{B} = \varepsilon \frac{\partial B}{\partial T_0} + \varepsilon^2 \frac{\partial B}{\partial T_1} + \mathcal{O}(\varepsilon^3), \tag{15}$$

where $\dot{A}$ and $\dot{B}$ are derivatives with respect to the original time t. In the above, $\partial A/\partial T_i$, $\partial B/\partial T_i$ for $i = 0, 1, \ldots$, are functions of A and B alone. Therefore,

$$\dot{A} = f_1(A, B; \varepsilon) \quad \text{and} \quad \dot{B} = f_2(A, B; \varepsilon). \tag{16}$$

The actual expressions involved, obtained here using the symbolic algebra package MAPLE, are long and not displayed. Instead, we now change variables in Equation (16) to polar coordinates:

$$A(t) = R(t) \cos(\phi(t)) \quad \text{and} \quad B(t) = R(t) \sin(\phi(t)).$$

Solving for $\dot{R}$ and $\dot{\phi}$, we get

$$\dot{R} = \frac{(2\pi - 3R^2) R}{\pi^2 + 4} \varepsilon$$
$$- \frac{[3R^4(7\pi^4 - 160\pi^2 + 16) + 288\pi R^2(\pi^2 - 4) + 32(\pi^4 + 12\pi^2 - 32)]\pi R}{32(\pi^2 + 4)^3} \varepsilon^2$$
$$+ \mathcal{O}(\varepsilon^3), \tag{17}$$

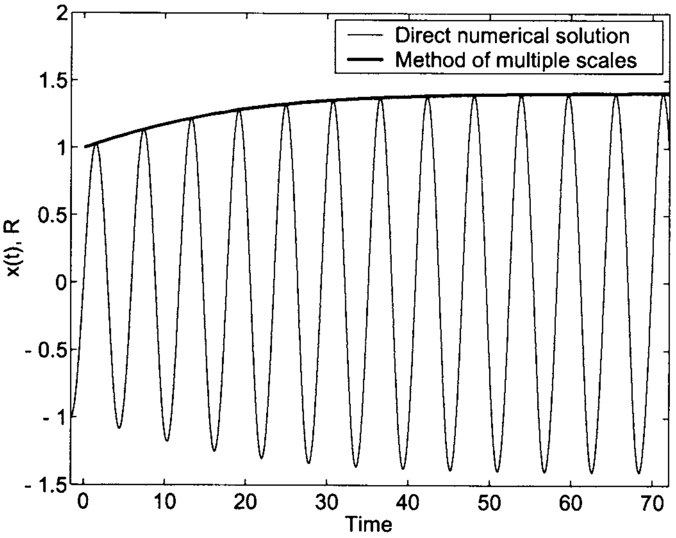

Figure 1. Numerical results from Equations (5) and (17) for $\varepsilon = 0.1$. Initial conditions: $x(\eta) = \sin\eta$, $\eta \in [-\pi/2, 0]$.

$$\dot{\phi} = \frac{1}{2}\frac{(3\,R^2\pi + 8)}{\pi^2+4}\,\varepsilon + \frac{24\pi^5R^2 - 32\pi^4 - 93R^4\pi^4 - 384R^2\pi^3 + 192R^4\pi^2 - 640\pi^2 + 384R^2\pi - 48R^4}{16(\pi^2+4)^3}\varepsilon^2 + \mathcal{O}(\varepsilon^3). \tag{18}$$

It is clear from the $\mathcal{O}(\varepsilon)$ terms in the equations above that, for small $\varepsilon > 0$, $R = 0$ is an unstable point, and there is a unique stable limit cycle (R constant).

Notice that, if we change variables to $p = R^2$ in Equation (17) and drop the $\mathcal{O}\left(\varepsilon^3\right)$ terms, it takes the form

$$\dot{p} = a\,p + b\,p^2 + c\,p^3, \tag{19}$$

which can be integrated analytically. Using that solution, Equation (18) can be solved as well. However, the expressions involved are somewhat long, and so in our comparisons with numerics below, we just integrate Equation (17) numerically.

To accurately obtain R for the limit cycle, we set $\dot{R}$ equal to zero in Equation (17), and solve for R in the form of a power series in ε:

$$R = \frac{\sqrt{6\pi}}{3} - \frac{\sqrt{6\pi}}{288}(7\pi^2 - 48)\,\varepsilon + \mathcal{O}(\varepsilon^2). \tag{20}$$

Substituting the above into Equation (18) and simplifying, we find

$$\dot{\phi} = \varepsilon - \frac{7\,\pi^2}{48}\,\varepsilon^2 + \mathcal{O}(\varepsilon^3). \tag{21}$$

The above expressions for R and $\dot{\phi}$ match those obtained using the Poincaré–Lindstedt method (see Appendix A). Equations (17) and (18), with terms included up to $\mathcal{O}(\varepsilon^3)$, were solved

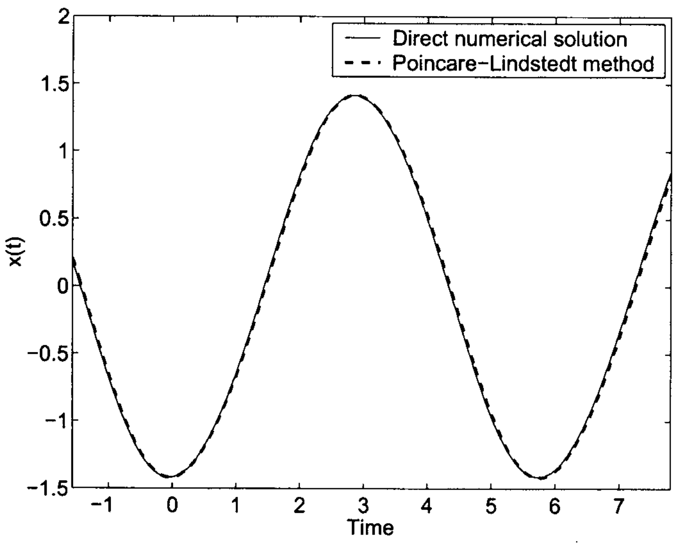

Figure 2. Periodic solutions of Equation (5), from numerics and Poincaré–Lindstedt, for $\varepsilon = 0.1$. The two solutions are shown slightly separated in time for easier comparison (the solutions remain valid because the DDE is autonomous).

using MATLAB's ODE solver (ode45). The results are compared in Figures 1 and 2 with (a) the direct numerical solution of the original DDE (using a fixed step[1] fourth order Runge–Kutta method adapted to include the delay term), and (b) the periodic solution from the Poincaré–Lindstedt method, respectively.

3. Weak Resonant Forcing near a Hopf Bifurcation

Now we consider Equation (5) with an added small forcing term:

$$\dot{x}(t) = -x(t - \frac{\pi}{2}) - \varepsilon \left[x\left(t - \frac{\pi}{2}\right) + x^3(t) - F \sin t \right]. \tag{22}$$

As for the previous example, MAPLE running on a PC easily carried out the multiple scales procedure up to third order (there is no limitation except in computer power; the calculation could be carried out to still higher orders if desired). The expressions for $\dot{R}$ and $\dot{\phi}$, where R and ϕ are as defined earlier, are lengthy and reproduced here only up to first order:

$$\dot{R} = \varepsilon \frac{(-2\pi F \sin\phi + 2\pi R + 4F\cos\phi - 3R^3)}{\pi^2 + 4}, \tag{23}$$

$$\dot{\phi} = -\varepsilon \frac{(4\pi F \cos\phi - 3\pi R^3 - 8R + 8F\sin\phi)}{2R(\pi^2 + 4)}. \tag{24}$$

However, the slow flow up to third order was used for the numerical results below.

Comparisons between the MMS and full numerical solutions are shown, for $\varepsilon = 0.1$, in Figures 3 and 4. As we decrease F from above a critical value ($F_c = 1.27984$ for $\varepsilon = 0.1$ in

[1] The time step used should be short enough so that significant high-frequency components do not get artificially suppressed. Infinitely many high frequencies will continue to elude numerics no matter how small the step size; however, their net contribution to the dynamics will be insignificant.

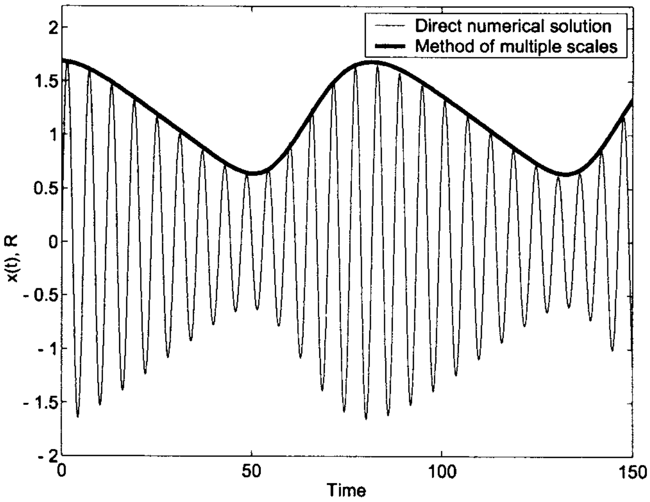

Figure 3. Smaller F, steady state behavior of Equation (22). Here, $\varepsilon = 0.1$ and $F = 1 < F_c = 1.27984$.

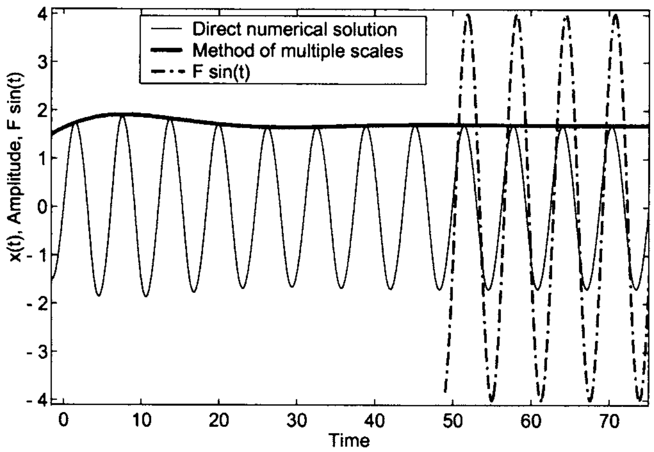

Figure 4. Larger F behavior of Equation (22). Here, $\varepsilon = 0.1$ and $F = 4 > F_c = 1.27984$. A few cycles of $F \sin t$ are plotted, showing that the response is phase locked to the forcing. Initial conditions: $x(\eta) = 1.5 \sin \eta$, $\eta \in [-\pi/2, 0]$.

this case), a supercritical Hopf bifurcation occurs when F crosses F_c (i.e., a stable fixed point bifurcates into an unstable fixed point and a stable limit cycle). For $F < 1.27984$ we observe modulated oscillating solutions with the amplitude itself oscillating as shown in Figure 3. This corresponds to a limit cycle solution in the original A-B variables. Stable fixed points are observed when $F > 1.27984$. This is shown in Figure 4 (for $F = 4$). The behaviors discussed above are shown in Figure 5 as well.

4. A Second Order Delay Differential Equation

For our third example, we consider the equation (taken from [6, 19])

$$\ddot{x}(t) + k\,\dot{x}(t) + x(t-\tau) + \theta^* x^3(t-\tau) = 0, \tag{25}$$

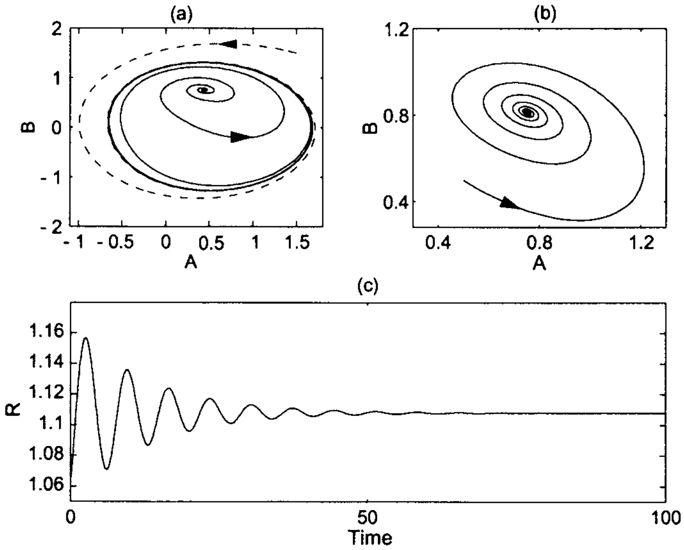

Figure 5. Behavior of Equation (22) for $\varepsilon = 0.1$. (a) A vs. B plane for $F < F_c$ ($F = 1$) shows an unstable fixed point and a stable limit cycle. (b) A vs. B plane for $F > F_c$ ($F = 1.5$) shows a stable fixed point. (c) R vs. time plot for $F = 1.5$ shows amplitude converging to the fixed point.

where $k > 0$, θ^* is a nonzero constant and τ is the time delay. The characteristic equation for the linearized form of Equation (25) is

$$\lambda^2 + k\,\lambda + \mathrm{e}^{-\lambda\,\tau} = 0. \tag{26}$$

It is known that (see [6]) the above equation will have purely imaginary roots $\pm i\,\omega$ if k and τ assume the critical values k_0 and τ_0 given by

$$k_0 = \sqrt{\frac{1-\omega^4}{\omega^2}} \quad \text{and} \quad \tau_0 = \frac{1}{\omega} \arctan \frac{k_0}{\omega}, \tag{27}$$

where we further require $0 < \omega < \min\{1, \pi/(2\,\tau_0)\}$.

In [6] it was demonstrated, with a center manifold construction and using normal forms, that a Hopf bifurcation occurs at $\tau/k = \tau_0/k_0$; the bifurcation is subcritical for $\theta^* > 0$ and supercritical for $\theta^* < 0$ (an anonymous reviewer has brought to our notice that the linear stability analysis of this system has also been addressed in [20]).

Among the three quantities k_0, τ_0 and ω in Equation (27), we can select a value for any one and subsequently determine the other two. Here we choose $\omega = 1/2$, and find $k_0 = 1.9365$, $\tau_0 = 2.6362$. Note that $0 < \omega < \pi/(2\,\tau_0) = 0.5959 < 1$ as required.

To study the system near the Hopf bifurcation, we now introduce a small parameter $0 < \varepsilon \ll 1$, set $k = k_0 + \varepsilon\,\Delta$, $\theta^* = \varepsilon\,\theta$ and $\tau = \tau_0$, and rewrite Equation (25) as

$$\ddot{x}(t) + (k_0 + \varepsilon\,\Delta)\,\dot{x}(t) + x(t-\tau_0) + \varepsilon\,\theta\,x^3(t-\tau_0) = 0. \tag{28}$$

In Equation (28), $\Delta = 0$ is the Hopf bifurcation point; the bifurcation is subcritical for $\theta > 0$ and supercritical for $\theta < 0$.

We again use MAPLE to carry out the MMS procedure for Equation (28) up to third order. The slow flow obtained is

$$\dot{R} = \left[0.16420\,\theta\,R^3 - 0.12463\,R\,\Delta\right]\varepsilon$$

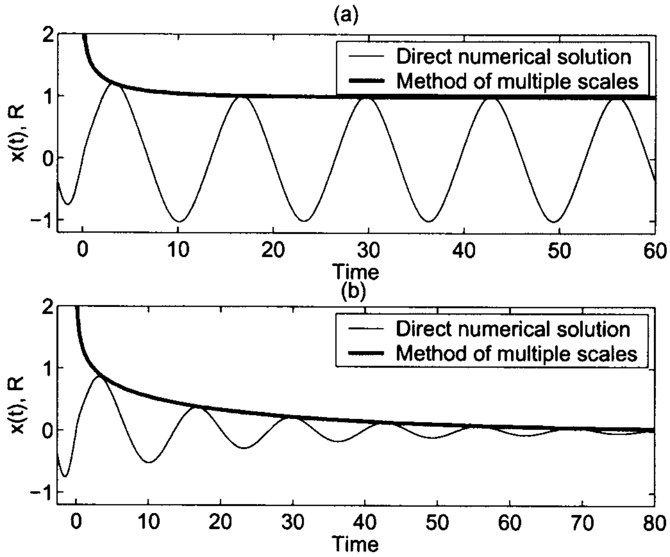

Figure 6. Comparison between numerics and MMS for Equation (28), with $\theta = -3$, $\varepsilon = 0.1$, and initial conditions $x(\eta) = 0.75 \sin \eta$, $\dot{x}(\eta) = 0.75 \cos \eta$, $\eta \in [-2.6362, 0]$. (a) $\Delta = -4$. (b) $\Delta = 3$.

$$+ \left[0.11191\, \theta\, R^3\, \Delta - 0.19904\, \theta^2\, R^5 + 0.02285\, R\, \Delta^2\right] \varepsilon^2$$
$$+ \left[0.01782\, \theta\, R^3\, \Delta^2 - 0.32632\, R^5\, \theta^2\, \Delta + 0.43375\, R^7\, \theta^3 - 0.00444\, R\, \Delta^3\right] \varepsilon^3, \quad (29)$$

and

$$\dot{\phi} = \left[0.11183\, \theta\, R^2 - 0.04482\, \Delta\right] \varepsilon$$
$$+ \left[-0.098512\, \theta^2\, R^4 + 0.05811\, \theta\, R^2\, \Delta - 0.00917\, \Delta^2\right] \varepsilon^2$$
$$+ \left[0.17503\, R^6\, \theta^3 - 0.17000\, R^4\, \theta^2\, \Delta + 0.03913\, \theta\, R^2\, \Delta^2 + 0.00355\, \Delta^3\right] \varepsilon^3, \quad (30)$$

where R and ϕ have the same meaning as earlier. In order to compare results with [6], we consider equilibria of the first order part of the R equation, given by

$$0.16420\, \theta\, R^3 - 0.12463\, R\, \Delta = 0. \quad (31)$$

There are now two cases.

If $\theta < 0$, the above equation has three real roots for $\Delta < 0$. Of the three, $R = 0$ is an unstable fixed point, while the other two represent a stable limit cycle. For $\Delta > 0$, $R = 0$ is the only root, and it is stable. Thus, the Hopf bifurcation is supercritical.

If $\theta > 0$, then the above equation has three real roots for $\Delta > 0$. Of the three, $R = 0$ is a stable fixed point, while the other two represent an unstable limit cycle. For $\Delta < 0$, $R = 0$ is the only root, and it is unstable. Thus, the Hopf bifurcation is subcritical.

The above observations agree with [6]. Numerical results (Figures 6 and 7) also show good agreement between multiple scales and numerical solutions.

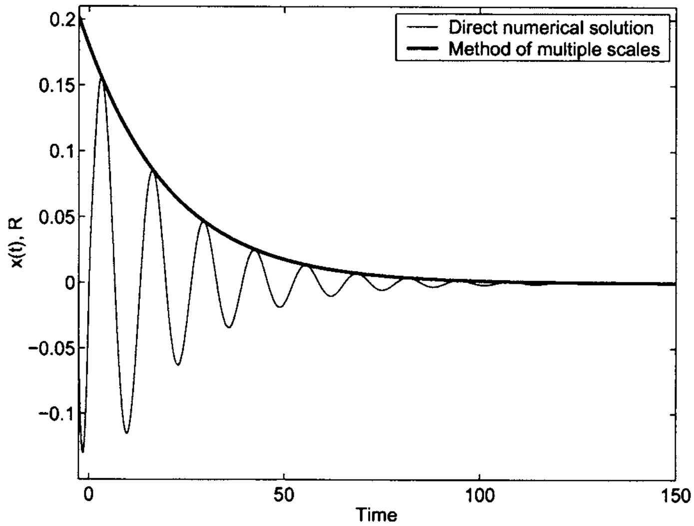

Figure 7. Comparison between numerics and MMS for Equation (28), with $\theta = 3$, $\Delta = 4$, $\varepsilon = 0.1$, and initial conditions $x(\eta) = 0.13 \sin \eta$, $\dot{x}(\eta) = 0.13 \cos \eta$, $\eta \in [-2.6362, 0]$.

5. Conclusions

We have studied delay differential equations near Hopf bifurcations. We have demonstrated that solutions obtained using the method of multiple scales (MMS) provide excellent approximations for the full numerical solutions of the original DDEs. Use of the MMS in these situations, along with simply discarding the infinitely many exponentially decaying components of the complementary solutions obtained at each stage of the approximation, eliminates the need for the explicit center manifold reduction recommended by several authors. This makes the analysis of DDEs near Hopf bifurcations similar to that of lower dimensional systems. With modern computer algebra programs, approximations to several orders can easily be obtained using the MMS via the straightforward procedure demonstrated in this paper.

Appendix A: Periodic Solution Using the Poincaré–Lindstedt Method

In the Poincaré–Lindstedt method we develop a period-amplitude relationship by stretching the time (for ODEs this method is discussed in [2, 3, 21]),

$$\tau = \omega t, \quad \text{where} \quad \omega = 1 + \varepsilon\, \omega_1 + \varepsilon^2 \omega_2 + \cdots, \tag{32}$$

and expressing x as

$$x(\tau) = x_0(\tau) + \varepsilon\, x_1(\tau) + \varepsilon^2\, x_2(\tau) + \cdots. \tag{33}$$

Substituting the above in Equation (5) and expanding in a Taylor series about $\varepsilon = 0$, at lowest order we get

$$\frac{\partial}{\partial \tau} x_0(\tau) + x_0\left(\tau - \frac{1}{2}\pi\right) = 0. \tag{34}$$

Equation (34) has the periodic solution (the sine term is dropped because the equation is autonomous)

$$x_0(\tau) = M \cos \tau. \tag{35}$$

At the next order we obtain an equation for x_1,

$$\begin{aligned} &\frac{\partial}{\partial t} x_1(\tau) \; + \; x_1\left(\tau - \frac{\pi}{2}\right) - (\omega_1 - 1)\, M \sin \tau \\ &\qquad + \; \left(\frac{3}{4} M^3 - \frac{1}{2} M\, \pi\, \omega_1\right) \cos \tau + \frac{1}{4} M^3 \cos 3\tau = 0. \end{aligned} \tag{36}$$

To avoid secular terms, we set the coefficients of $\sin \tau$ and $\cos \tau$ to zero, obtaining

$$M = \frac{\sqrt{6\pi}}{3}, \quad \omega_1 = 1,$$

and

$$\frac{\partial}{\partial t} x_1(\tau) + x_1\left(\tau - \frac{\pi}{2}\right) + \frac{1}{4} M^3 \cos 3\tau = 0. \tag{37}$$

We assume the homogeneous solution to the above equation as

$$x_{1h}(\tau) = N \sin \tau \tag{38}$$

(note that we do not need to keep the cosine because that has been included at the leading order; see discussion below) and also obtain a particular solution as

$$x_{1p} = -\frac{\sqrt{6\pi}}{72}\, \pi \sin 3\tau.$$

Substituting the above results into the original equation, we obtain at $\mathcal{O}(\varepsilon^2)$ an equation for x_2. There, elimination of secular terms gives

$$N = -\frac{\sqrt{6\pi}\,(7\pi^2 - 48)}{288} \quad \text{and} \quad \omega_2 = -\frac{7\pi^2}{48}.$$

At this point, we have

$$x(\tau) = \frac{\sqrt{6\pi}}{3} \cos \tau - \frac{\sqrt{6\pi}}{72} \left(\frac{7\pi^2 - 48}{4} \sin \tau + \pi \sin 3\,\tau\right) \varepsilon + \mathcal{O}(\varepsilon^2), \tag{39}$$

and

$$\omega = 1 + \varepsilon - \frac{7\,\pi^2}{48}\, \varepsilon^2 + \mathcal{O}(\varepsilon^3). \tag{40}$$

The above expansions could in principle be carried out to any order desired.

From the above results, we obtain

$$R = \frac{\sqrt{6\pi}}{3} + \mathcal{O}(\varepsilon) \quad \text{and} \quad \dot{\phi} = \varepsilon - \frac{7\,\pi^2}{48}\, \varepsilon^2 + \mathcal{O}(\varepsilon^3).$$

Note that the value obtained here for R is difficult to compare, except at leading order, with the value obtained previously using multiple scales. This is because of the nonuniqueness of the expansion. Inclusion of an arbitrary cosine term in Equation (38) would change the R values arbitrarily at higher orders. Note, however, that the crucial match is in the time periods obtained from the two methods (multiple scales and Poincaré–Lindstedt); the two solutions for time periods will match to all orders regardless of whether or not we include cosine terms in Equation (38) and its higher order counterparts. Thus, based on the match in time periods, we can say that MMS matches Poincaré–Lindstedt.

Acknowledgements

This work was partially supported through a joint grant from ISRO and DRDO for the Nonlinear Studies Group at the Indian Institute of Science. Richard Rand outlined the Poincaré–Lindstedt method for DDEs and mentioned the integrability of Equation (17). Two anonymous reviewers provided several useful comments as well as references.

References

1. Hinch, E. J., *Perturbation Methods*, Cambridge University Press, Cambridge, 1991.
2. Kevorkian, J. and Cole, J. D., *Multiple Scales and Singular Perturbation Methods.* Springer-Verlag, New York, 1996.
3. Nayfeh, A. H., *Introduction to Perturbation Techniques*, Wiley, New York, 1981.
4. Campbell, S. A., Bélair, J., Ohira, T., and Milton, J., 'Complex dynamics and multistability in a damped harmonic oscillator with delayed negative feedback', *Chaos* **5**(4), 1995, 640–645.
5. Fofana, M. S., 'A unified framework for the study of periodic solutions of nonlinear delay differential equations', in *Proceedings of the DETC'01, ASME 2001 Design Engineering Technical Conference and Computers and Information in Engineering Conference*, Pittsburgh, PA, Paper No. DETC2001/VIB21617, ASME, New York, 2001, pp. 1–20.
6. Xu, J., and Lu, Q. S., 'Hopf bifurcation of time-delay Lienard equations', *International Journal of Bifurcation and Chaos* **9**(5), 1999, 939–951.
7. Wang, Z. H. and Hu, H. Y., 'Dimensional reduction for nonlinear time-delayed systems composed of stiff and soft substructures', *Nonlinear Dynamics* **25**, 2001, 317–331.
8. Stepan, G., 'Modelling nonlinear regenerative effects in metal cutting', *Philosophical Transactions of the Royal Society of London* **359**, 2001, 739–757.
9. Stepan, G. and Kalmar-Nagy, T., 'Nonlinear regenerative machine tool vibrations', in *Proceedings of ASME Design Engineering Technical Conference on Vibration and Noise*, Sacramento, CA, Paper No. DETC97/VIB-4021, ASME, New York, 1997, pp. 1–11.
10. Pai, P. F. and Nayfeh, A. H., 'Non-linear non-planar oscillations of a cantilever beam under lateral base excitations', *International Journal of Non-Linear Mechanics* **25**(5), 1990, 455–474.
11. Chin, C. and Nayfeh, A. H., 'Three-to-one internal resonances in parametrically excited hinge-clamped beams', *Nonlinear Dynamics* **20**(2), 1999, 131–158.
12. Faria, T. and Magalhaes, L. T., 'Normal forms for retarded functional differential equations and applications to Bogdanov-Takens singularity', *Journal of Differential Equations* **122**, 1995, 201–224.
13. Faria, T. and Magalhaes, L. T., 'Normal forms for retarded functional differential equations with parameters and applications to Hopf bifurcation', *Journal of Differential Equations* **122**, 1995, 181–200.
14. Faria, T., 'Normal forms for periodic retarded functional differential equations', *Proceedings of the Royal Society of Edinburgh* **127A**, 1997, 21–46.
15. Moiola, J. L., Chiacchiarini, H. G., and Desages, A. C., 'Bifurcations and Hopf degeneracies in nonlinear feedback systems with time delay', *International Journal of Bifurcation and Chaos* **6**(4), 1996, 661–672.
16. Plaut, R. H. and Hseih, J. C., 'Non-linear structural vibrations involving a time delay in damping', *Journal of Sound and Vibration* **117**(3), 1987, 497–510.

17. Hu, H. Y., Dowell, E. H., and Virgin, L. N., 'Resonances of a harmonically forced Duffing oscillator with time delay state feedback', *Nonlinear Dynamics* **15**, 1998, 311–327.
18. Maccari, A., 'The response of a parametrically excited van der Pol oscillator to a time delay state feedback', *Nonlinear Dynamics* **26**, 2001, 105–119.
19. Hale, J. K. and Lunel, S. V., *Introduction to Functional Differential Equations*, Springer-Verlag, New York, 1993.
20. Stepan, G., *Retarded Dynamical Systems*, Longman, Harlow, 1989.
21. Rand, R. H., *Lecture Notes on Nonlinear Vibrations*, Version 36, available online at http://tam.cornell.edu/randdocs/nlvibe36.pdf, 2001.